

THE TUMBLING MOON: ROTATIONAL DYNAMICS IN THE AFTERMATH OF IMPACT BASIN FORMATION. J. T. Keane¹, B. C. Johnson², I. Matsuyama³ and M. A. Siegler^{4,5}, ¹California Institute of Technology, Pasadena, CA 91125, USA (jkeane@caltech.edu); ²Department of Earth, Environmental and Planetary Sciences, Brown University, Providence, RI 02912, USA; ³Lunar and Planetary Laboratory, University of Arizona, Tucson, AZ 85721, USA; ⁴Planetary Science Institute, Tucson, AZ 85719, USA; ⁵Southern Methodist University, Dallas, TX 75275, USA.

Introduction: The spins of planets are not constant with time; they change in response to both external and internal forces on a variety of spatial and temporal scales. One of the most dramatic ways a planet’s spin can change is via impacts. Impacts change a planet’s angular momentum, rotational energy, and moments of inertia. These changes can have a variety of important consequences for the geology of the planet, including unlocking tidally-locked satellites [1], stirring up the core dynamo [2], generating tectonic stresses in the crust [3], and altering the stability of water and other volatiles in permanently shadowed regions [4].

While several previous studies have investigated the dynamical effects of impacts on the Moon, most use simplified models for the impact basin formation process—often only considering the (small) impulsive change in the Moon’s angular momentum, and (occasionally) the change in the Moon’s moments of inertia from a simplified basin geometry (e.g. a cylindrical hole in the ground) [1, 5-7]. However, our understanding of the impact basin formation process has dramatically improved in the past decade thanks to new geophysical measurements from NASA’s GRAIL and LRO missions [8], and new numerical simulations of the impact process [9]. In this work, we leverage these recent advances and reexamine the rotational dynamics of the Moon in the aftermath of large impacts. We find that that moment of inertia perturbations from impacts are significantly larger than previously expected, and the resulting rotational dynamics of the Moon is far more dramatic than previously recognized.

The Change in the Moon’s Moments of Inertia

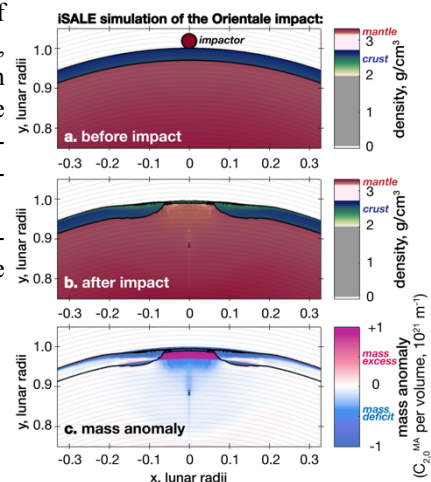
After Impact: One of the largest uncertainties in the rotational dynamics a planet after impact is how its moments of inertia change after impact. While the present-day gravity field allows us to quantify the present-day moment of inertia perturbations associated with impact basins [10], these perturbations do not necessarily reflect the *initial* moment of inertia perturbations. Basins relax and change their structures in a variety of ways after impact [11-12]. To investigate the rotational dynamics of the Moon after impact, we use state-of-the-art iSALE hydrocode simulations [13-15] to quantify the moment of inertia perturbations of fresh impact basins. iSALE allow us to quantitatively track how different impact processes alter the Moon’s moments of inertia,

including basin excavation, mantle uplift, impact heating, and ejecta blanket emplacement.

Figure 1 shows an example iSALE simulation of the formation of the Orientale impact basin [9]. We calculate the total moment of inertia perturbation from the basin by summing the change in moments of inertia due to the change in density in each grid-cell. Because our iSALE simulations are axisymmetric, this perturbation can be reduced to a single quantity which we term the “mass anomaly,” $C_{2,0}^{MA}$. The mass anomaly is the degree-2 zonal spherical harmonic gravity coefficient ($C_{2,0} = -J_2$) associated with the fresh impact basin.

Our iSALE simulations reveal that Orientale was initially a large negative mass anomaly ($C_{2,0}^{MA} \sim -50 \times 10^{-6}$), roughly $\sim 25\%$ of the Moon’s present-day dynamical oblateness ($C_{2,0}^{Moon} \sim -200 \times 10^{-6}$). This contrasts with the small, positive, present-day mass anomaly measured by GRAIL ($C_{2,0}^{MA} \sim 20 \times 10^{-6}$) [10]. This difference arises from the relaxation and shallowing of the deep, strongly subsostatic basin in the Myr following the impact [11-12]. Most of this initial mass anomaly comes from the topography of the fresh basin, which is much deeper than the present-day basin. Other processes—like crustal thickening and mantle heating—play a minor role.

Fig. 1: iSALE simulation of the formation of the Orientale impact basin.



Our iSALE simulations of the gigantic South Pole-Aitken (SP-A) impact basin reveal even more dramatic results. The mass anomaly of early SP-A far exceeded the dynamical oblateness of the present-day Moon ($C_{2,0}^{MA} \sim -400 \times 10^{-6} \sim 2C_{2,0}^{Moon}$)! Thus, for a time, the rotation of the Moon was controlled by SP-A.

Rotational Dynamics of the Moon Post Impact:

The large instantaneous change in the Moon’s moments of inertia after impacts results in complicated rotational motion. While the angular momentum vector of the

Moon is only weakly perturbed by an impact [5], the orientation of the Moon's principal axes of inertia can change substantially—misaligning the principal axes with both the angular momentum vector and the tidal vector. This misalignment results in rotation about each of the three principal axes of inertia, i.e., a non-principal axis (“tumbling”) rotation state. Many comets are observed to tumble (due to outgassing torques), as are some small, eccentric moons subject to strong tidal torques (e.g. Hyperion). To track the rotation of the Moon after impacts, we numerically integrate Euler's equations of motion in the body-fixed reference frame [16-19].

Figure 2 shows examples of the spin of the Moon after the formation of the Orientale and SP-A impact basins. Both impacts result in significant, different styles of tumbling. Orientale's mass anomaly is smaller than the Moon's dynamical figure, and results in large amplitude librations ($\sim 50^\circ$; Fig. 2a) and polar motions ($\sim 30^\circ$; Fig. 2b). We expect other comparably sized impact basins (Imbrium, Serenitatis, etc.) will result in similar large-scale librations. SP-A is large enough that it breaks the Moon out of synchronous tidal lock (Fig. 2d). An observer on the Hadean Earth would be able to see both faces of the Moon for a time after impact (although they may have other things to worry about; Fig. 2f). While tidal-unlocking has been hypothesized for the largest impact basins based on the torque imparted by impact [1, 5-7], this is a wholly new mechanism for tidal-unlocking—arising solely from the change in orientation of the principal axes of inertia.

Implications: These episodes of impact-induced tumbling have important consequences for a variety of geologic processes. For example, previous work has suggested that the spatial distribution of lunar polar volatiles record an early epoch of lunar true polar wander [4]. Our work has shown that the formation of impact basins induced wobbles large enough ($>12^\circ$ [20]; Fig. 2b) to expose most permanently shadowed regions to direct sunlight and volatile loss. Thus, we can bracket the age of polar volatiles to be no older than the last large impact basin (likely Orientale at 3.8 Ga).

While our work focuses on the Moon, the dynamical processes presented here are incredibly general, and likely apply to a variety of solar system worlds. Worlds with smaller differences between principal moments of inertia (e.g. Mercury, some icy satellites) will be more susceptible to these impact-induced tumbles.

Acknowledgments: We gratefully acknowledge the developers of iSALE-2D, including Gareth Collins, Kai Wünnemann, Dirk Elbeshausen, Boris Ivanov and Jay

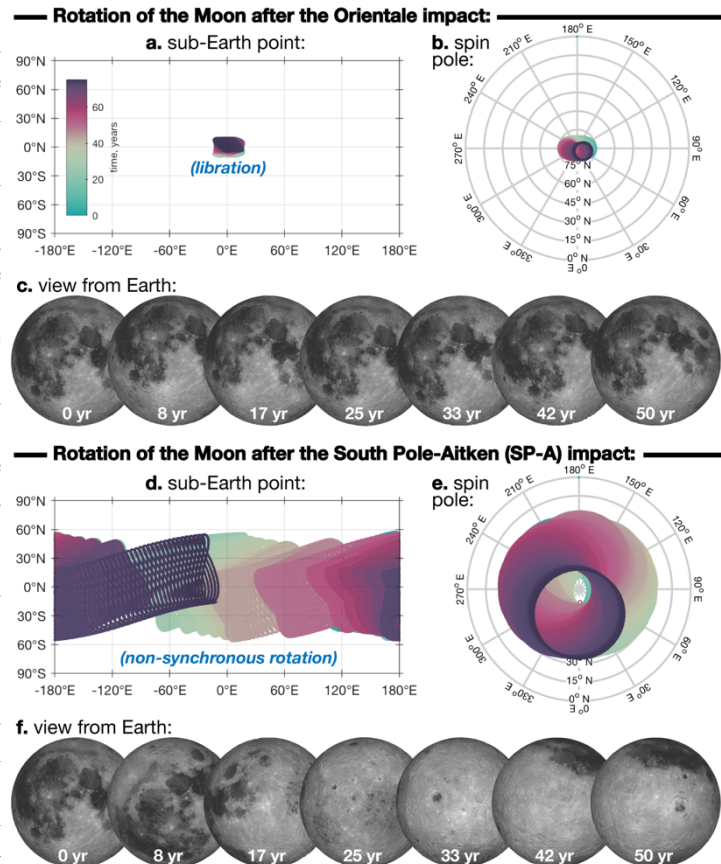


Fig. 2: Dynamics of the Moon in the aftermath of large impacts (neglecting impact torques)

Melosh. This work was funded by the Caltech JCPA fellowship and NASA Solar System Workings program (NNX16AQ05G, PI: Keane).

References: [1] Encore, M. A. & Le Feuvre, M. (2009) *Icarus*, 200, 358-366. [2] Le Bars, M. et al. (2011) *Nature*, 479, 215-218. [3] Keane J. T. et al. (2016) *Nature*, 540, 90-93. [4] Siegler, M. A. et al. (2016) *Nature*, 531, 480-484. [5] Melosh, H. J. (1975) *EPSL*, 26, 353-360. [6] Peale, S. J. (1985) *JGR*, 80, 4939-4946. [7] Lissauer, J. J. (1985) *JGR*, 90, 11289-11293. [8] Zuber, M. T. et al. (2016) *Science*, 354, 438-441. [9] Johnson, B. C. et al. (2016) *Science*, 354, 441-444. [10] Keane, J. T. & Matsuyama, I. (2014), *GRL*, 41, 6610-6619. [11] Melosh, H. J. et al. (2013) *Science*, 340, 1552-1555. [12] Freed, A. M. et al. (2014) *JGR: Planets*, 119, 2378-2397. [13] Amsden, A. et al. (1980) *LANL Report*, LA-8095. [14] Collins, G. S. et al. (2004) *MAPS*, 38, 217-231. [15] Wünnemann, K. et al. (2006) *Icarus*, 180, 514-527. [16] Wisdom, J. et al. (1984) *Icarus*, 58, 137-152. [17] Klavetter, J. J. (1989) *AJ*, 98, 1855-1874. [18] Black, G. J. et al. (1995) *Icarus*, 117, 149-161. [19] Harbison, R. A. et al. (2011) *CMDA*, 110, 1-16. [20] Siegler, M. A. et al. (2015) *Icarus*, 255, 78-87.